Experimental Investigation on the Health Monitoring of Fluid Dampers for Bridges

Konstantinidis, Dimitrios
McMaster University, Hamilton, Canada

Makris, Nicos
University of Patras, Greece

Kelly, James M.
University of California, Berkeley, USA

SUMMARY
This paper presents results from a comprehensive experimental program on medium-size and large-size fluid dampers in an effort to extract their force output during cyclic loading by simply measuring the strain on the damper housing and the end-spacer. The paper first discusses the stress path within the damper and subsequently via the use of linear elasticity shows that the experimental data obtained with commercially available strain gauges yield a force output of the damper that is in good agreement with the readings from the load cell. The paper then examines the performance of a portable data acquisition system that can be used to collect and transmit data from a damper installed on a bridge to a nearby location. The data show that the proposed arrangement is promising for monitoring in-situ the force output of fluid dampers and detecting possible loss of their energy dissipation capability.

Keywords: health monitoring, remote sensing, fluid dampers

1. INTRODUCTION

The rapid success of fluid dampers as seismic protection devices, in association with the increasing need for safe bridges, has accelerated the implementation of large-capacity damping devices in bridges. For instance, the Vincent Thomas suspension bridge, the Coronado bridge and the 91/5 highway overcrossing (Delis et al. 1996, Makris and Zhang 2004), all three in southern California, the San Francisco–Oakland Bay Bridge and the Richmond–San Rafael bridge in northern California, as well as the Rion–Antirion cable-stayed bridge (Papanikolas 2002) in western Greece are all examples of bridges that have been equipped with fluid dampers.

The main challenge with fluid dampers is whether they will maintain their long-term integrity when placed in such large structures which are subjected to a variety of loads, appreciable dynamic displacements and long-term deformation patterns. Whereas large displacements and velocities are expected during earthquake loading, a prolonged wind loading would increase substantially the temperature of the damper. Similarly, traffic loading which induces vibrations of small amplitude but very long duration may fatigue the damper and eventually be detrimental, as was experienced with the fluid dampers installed in the Vincent Thomas Bridge in southern California and the San Francisco–Oakland Bay Bridge in northern California.

In this paper we present a comprehensive experimental investigation into the development and validation of simple and reliable technologies to monitor and transmit the force output and velocity histories of a fluid damper when installed in the field.

Experiments were conducted on two medium-size and two large-size fluid dampers at the Earthquake Simulator Laboratory of the Pacific Earthquake Engineering Research (PEER) Center, University of California, Berkeley. Fig. 1(left) shows one of the two medium-size dampers, which are identical to the fluid dampers installed in the 91/5 over-crossing in Orange Country, California (maximum stroke

= ±20.3 cm with maximum force output = 1100 kN at 107 cm/s piston velocity) (Delis et al. 1996, Makris and Zhang 2004). In addition to the two medium-size dampers, two larger fluid dampers (maximum stroke = ±48.3 cm with maximum force output = 2000 kN at 216 cm/s piston velocity) were tested, as shown in Fig. 1(right). These larger dampers are the same type of dampers as those installed at the west span of the San Francisco–Oakland Bay Bridge.

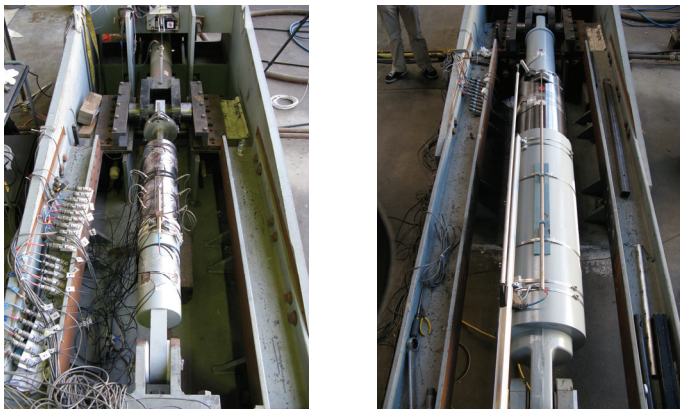

Figure 1. Left: 1100-kN damper. Right: 2000-kN damper; both tested at PEER Center laboratory, UC Berkeley

The first series of tests were conducted at the PEER laboratory using the damper testing machine shown in Fig. 1. These tests included a wide range of combinations of displacements and velocities in order to examine the fidelity and dependability of using bondable and weldable strain gauges, as well as displacement/velocity transducers, to estimate the force output of a damper. The force output computed from the strain gauges and the displacement/velocity transducers was compared with the force output from the load cell.

After the first series of component tests was completed indoors, a 2000-kN damper was moved outside of the laboratory and was mounted on a surplus test frame (Fig. 2). Since the facility is on the edge of the San Francisco Bay, the damper was exposed to environmental conditions typical of an actual field installation. The condition of the damper and the various transducers over time were remotely (using cables) assessed from inside the laboratory. The damper was cycled continuously an average of ten hours per day at low displacements and frequencies, typical of what would be expected in the field. At the end of the outdoor tests, the cumulative stroke on the damper had exceeded 8.85 km.

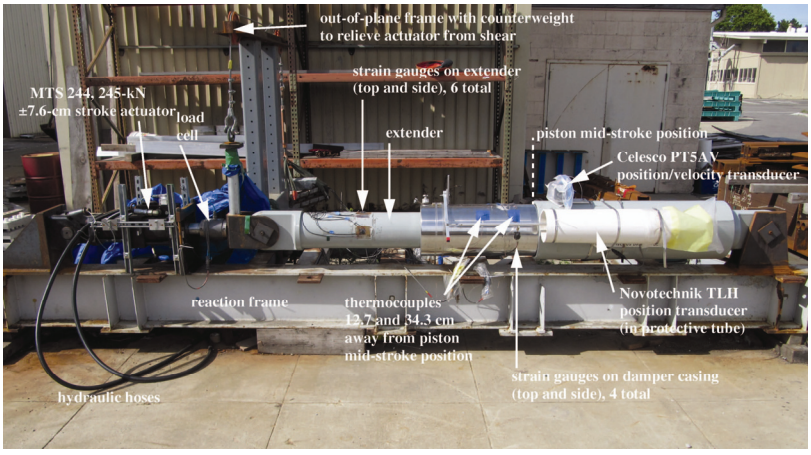

Figure 2. View of the fully instrumented 2000-kN damper mounted on the outdoor testing machine at PEER

During the experimental effort, the issue of transmitting data wirelessly to a nearby recording center was investigated. We examined how recent advances in technology can be applied to the health

monitoring of fluid viscous dampers in bridges. Using commercially available electronic components manufactured by Opto 22, we built a portable data acquisition system that can be used to collect and transmit data from a damper on a bridge to a nearby location using wireless communication (Wi-Fi). Alternatively, the data may be transmitted to any remote location via a Global System for Mobile Communications (GSM, or by its successors: 3G or 4G).

2. PATH OF STRESSES DURING CYCLIC LOADING OF FLUID DAMPERS AND MEASUREMENT OF THE FORCE OUTPUT FROM THE DAMPER CASING

Figure 3 shows schematically the stressing of the damper casing during tension and compression of the piston rod. When the piston rod is in tension, shown in Fig. 3(a), the damper casing is subjected to longitudinal tension; while, when the piston rod is in compression, shown in Fig. 3(b), the compressive force is transferred directly to the extender via the pressurized fluid at the back chamber; therefore, only tangential (hoop) stresses develop during the bursting of the damper.

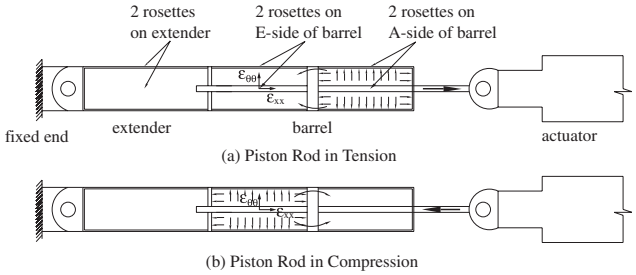

Figure 3. Cross section of a fluid damper showing the stressing of the damper casing during (a) tension of the piston rod, (b) compression; together with the principal strains ε_{xx} and $\varepsilon_{\theta\theta}$ that develop on the cylinder

The central idea of this work is to use standard strain gauges to monitor the force output of fluid dampers. The damper housing is merely a steel cylinder that is intended to be loaded along its principal direction; therefore, when appropriately instrumented, it resembles a load cell. Assuming that the attachments of the damper are perfectly aligned, the principal directions of deformation are the longitudinal direction (x-x) and the tangential direction (θ-θ) of the cylindrical housing, as shown in Fig. 3 on the side of the damper casing closer to the extender. In this case, strain gauges are placed along the principal directions, and direct measurements of ε_{xx} and $\varepsilon_{\theta\theta}$ are obtained. The principal stresses, σ_{xx} and $\sigma_{\theta\theta}$ may then be calculated from Hooke's law

$$\sigma_{xx} = \frac{E\left(\varepsilon_{xx} + \nu\varepsilon_{\theta\theta}\right)}{1-\nu^2}; \quad \sigma_{\theta\theta} = \frac{E\left(\varepsilon_{\theta\theta} + \nu\varepsilon_{xx}\right)}{1-\nu^2} \tag{2.1}$$

where E and ν are the Young's modulus and Poisson's ratio of the steel of the damper housing. The force output of the damper in terms of the experimentally measured strains is

$$P = A\sigma_{xx} = \frac{\pi}{4}\left(d_o^2 - d_i^2\right)\frac{E\left(\varepsilon_{xx} + \nu\varepsilon_{\theta\theta}\right)}{1-\nu^2} \tag{2.2}$$

where d_o and d_i are the outer and inner diameters of the damper housing. Table 1 offers the pertinent geometrical and mechanical characteristics (Zhang et al. 2004, Konstantinidis et al. 2011) of the two dampers tested in this work. In the event that installation imperfections are present, shear forces and bending moments may develop along the damper casing. In this case, the entire strain field may be measured by strain gauge rosettes.

In addition to the strain measurements which will yield directly the measured forces that develop in the dampers, measurement of the piston's velocity are needed. This can be either recovered by

differentiating the displacement signal measured using a standard Linear Variable Displacement Transducer (LVDT) or obtained directly with commercially available velocity transducers. Velocity transducers designed to operate in harsh marine environments are commercially available. Further details on the instrumentation used in this project are offered later.

Table 1. Geometrical and mechanical characteristics of the two dampers considered in this study

Quantity	1100-kN damper	2000-kN damper
Damping coefficient, C_α	217 kN(s/cm)$^{0.35}$	399 kN(s/cm)$^{0.30}$
Exponent, α	0.35	0.30
Outer diameter of damper housing, d_o [cm]	20.8	35.2
Inner diameter of damper housing, d_i [cm]	14.9	25.9
Rod diameter, d_r [cm]	5.66	9.45
Area of piston head, A_p [cm^2]	149	457
Maximum stroke, U_0 [cm]	±20.3	±48.3
Cross-sectional area of extender, A_e [cm^2]	230	368

With the actual (measured) piston velocity $\dot{u}(t)$ available, the expected (theoretical) force output is

$$\bar{P}(t) = C_\alpha \left|\dot{u}(t)\right|^\alpha \operatorname{sgn}\left[\dot{u}(t)\right] \tag{2.3}$$

The expected force output of the damper will then be compared with the experimentally measured force output of the damper given by Eqn. (2.2), and one can directly detect if there is an appreciable drop in the damper force. In the event that a large drop in force between these two, $\Delta P = \bar{P}(t) - P(t)$, (or between $\bar{P}(t)$ and the experimental force obtained during the production tests at the same piston velocity) is detected, say more than 15%, then one can pronounce the damper damaged. Of course, the fidelity of the theoretical force output is expected to have been validated during the production tests of the dampers. Furthermore, if the drop in force increases with the number of cycles, then the damage will be considered significant, and the damper will need to be replaced. Alternatively, under cyclic loading, any significant deviation in shape of the recorded force–displacement loops from the anticipated force–displacement loops established during production testing can be examined, and damage can be assessed based on the distortion of the loops rather than the percentage of force drop.

3. EXPERIMENTAL PROGRAM

3.1. 1100-kN Damper with Bondable Strain Gauges

One of the two available medium-size, 1100-kN fluid dampers was tested first. The damper was equipped with conventional, adhesive-bonded strain gauges. A total of six strain-gauge rosettes were bonded on the specimen. Figure 4 shows a rosette bonded on the side of the damper casing closer to the extender (referred to herein as *E-side*) and a rosette bonded on the side of the damper casing closer to the actuator (*A-side*). Two more rosettes that are not visible in the photograph are bonded on the bottom of the damper casing, i.e., at 90 degrees, one on the E-side and one on the A-side. Figure 5 shows a close-up view one of two rosettes that were bonded on the extender.

The relative displacement between the actuator clevis and a stationary point on the reaction frame was measured using a ±7.6-cm Transtek Series 240 DCDT displacement transducer. This will henceforth be referred to as the *actuator displacement*. Another ±7.6-cm Transtek transducer was used to measure the relative displacement between a point on the damper cover and a point on the damper barrel. This will henceforth be referred to as the *damper displacement*.

The 1100-kN damper with bonded strain gauges was subjected to sinusoidal signals with various displacement amplitudes (ranging from 0.127 to 6.35 cm) and frequencies (from 0.25 Hz to 2 Hz), corresponding to velocity amplitudes v_0 ranging between 0.76 cm/s to 59.9 cm/s.

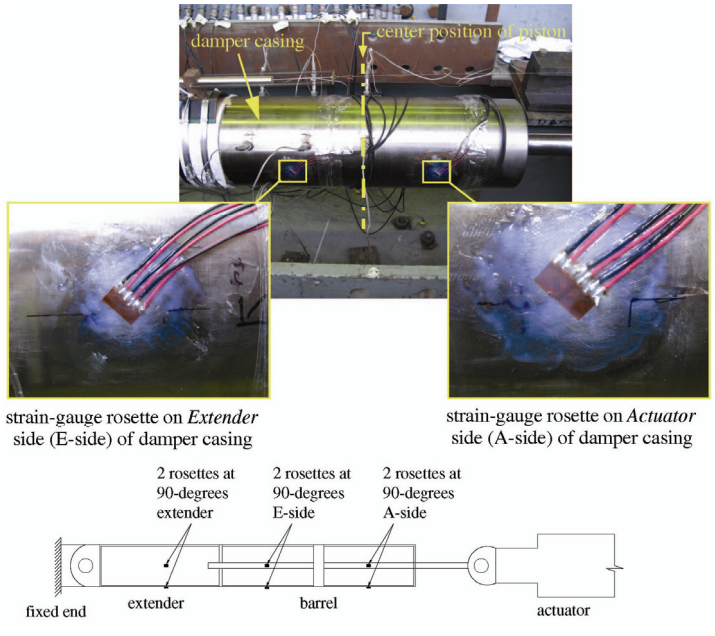

Figure 4. Strain-gauge rosettes on the casing of the 1100-kN damper

Figure 5. Strain-gauge rosette on the extender of the 1100-kN damper

Figure 6 shows selected results of tests conducted on the 1100-kN damper equipped with bondable strain-gauge rosettes. The left column shows graphs of results that were obtained from strain-gauge rosettes bonded on the damper casing, as shown in Fig. 4. The right column shows graphs of results obtained from rosettes bonded on the extender, as shown in Fig. 5. The bottom-right corner of the figure serves as a legend explaining what each curve represents. The displacement time histories shown are obtained from DCDTs attached on the damper and the actuator. In general, there is good agreement between the two recorded signals, except for differences attributed to slack (play) in the actuator and damper clevises and deformation of the testing machine. These differences are less pronounced for large-amplitude signals, implying that they are mostly caused by play in the clevises.

A total of 18 strain gauge channels (six rosettes) were recorded during the tests. On the left column, the graphs labelled ε_{xx} and $\varepsilon_{\theta\theta}$ are the longitudinal and hoop strains recorded on the A-side and E-side (Fig. 4). Figure 6 (left) confirms that the damper casing is stressed only when the piston rod is in tension (see Fig. 3), while when the piston rod is in compression, the damper casing experiences little axial deformation due to the Poisson effect from the hoop strains. On the other hand, Fig. 6 (right) indicates that when the strain gauges are installed on the extender, Eqn. (2.2) predicts with remarkable accuracy the force recorded from the load cell.

3.2. 1100-kN Damper with Weldable Strain Gauges

The second of the two available 1100-kN fluid dampers was equipped with Micro-Measurements CEA-06-W250A-120 weldable strain gauges. These types of strain gauges are factory-prebonded with

a high-performance adhesive to thin metal carriers. The metal carriers are spot welded around their perimeter to the specimen using a portable stored-energy hand-probe welder, as shown in Fig. 7(a). Weldable strain gauges are advantageous to bondable strain gauges in a bridge application because for the former the specimen requires minimal surface preparation; only a solvent cleaning and abrasion of the test surface with sandpaper or a small hand-held grinder is necessary. The welding unit incorporates a soldering gun to connect wires to terminals of the strain gauge. Lastly, protective coatings can be easily applied on the strain gauge to protect it against the harsh marine environment of a bridge. For example, a Vishay Micro-Measurements M-Coat A, followed by M-Coat B or M-Coat C, followed by M-Coat J will provide sufficient protection for the strain gauge.

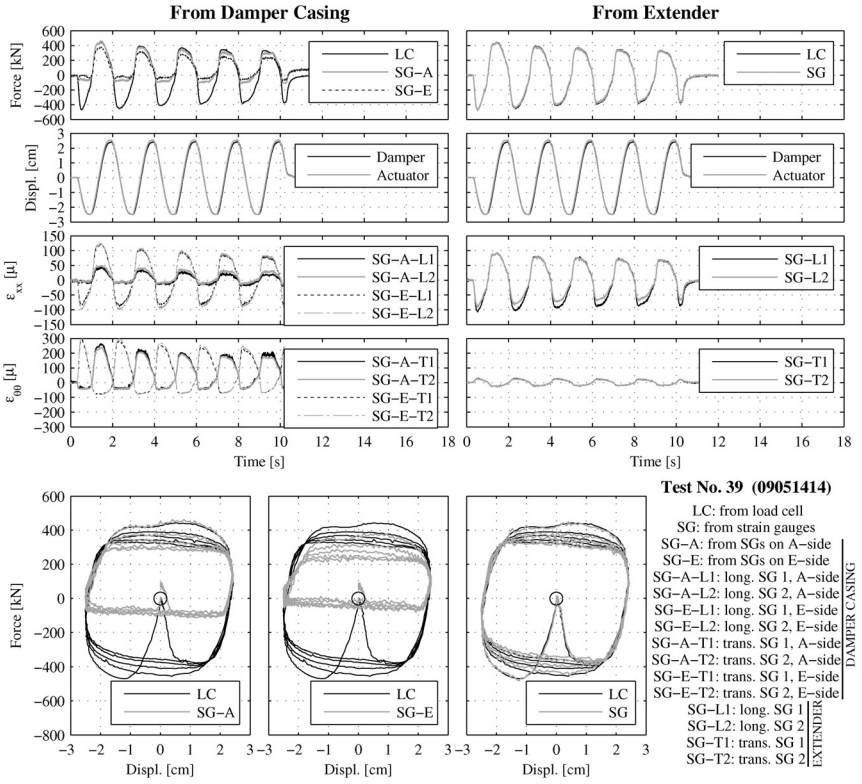

Figure 6. Recorded data from the 1100-kN damper equipped with bondable strain gauges

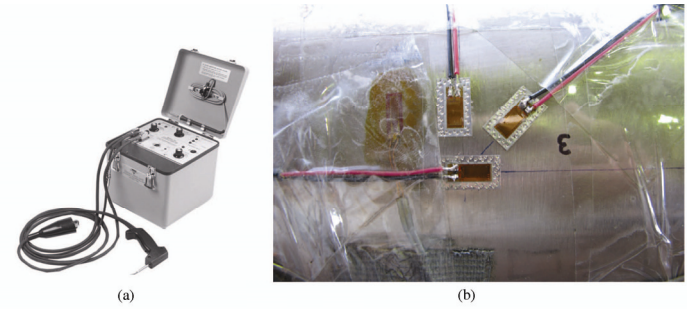

Figure 7. (a) Vishay Micro-Measurements 700 portable strain-gauge welding and soldering unit. (b) A built-up rosette of weldable strain gauges

Figure 7(b) shows one of several built-up rosettes consisting of weldable strain gauges. The arrangement of strain-gauge rosettes on the second 1100-kN damper is equivalent to that shown in Fig. 4 for the bondable strain-gauge rosettes. Data from a total of 18 strain gauge channels (six rosettes) were collected. It is important to note that, as the experiments confirmed, the use of this many strain

gauges is unnecessary because there is a large degree of redundancy in the data collected. As for the tests on the damper equipped with bondable strain gauges, the actuator and damper displacements was measured using two ±7.6-cm Transtek Series 240 DCDT displacement transducers.

Figure 8 compares the force output of the damper as predicted from Eqn. (2.2), where the strains ε_{xx} and $\varepsilon_{\theta\theta}$ are measured on the extender of the damper together with the force output from the load cell. The comparison of the results is remarkable for both the moderate- (left column) and high-force (right column) output.

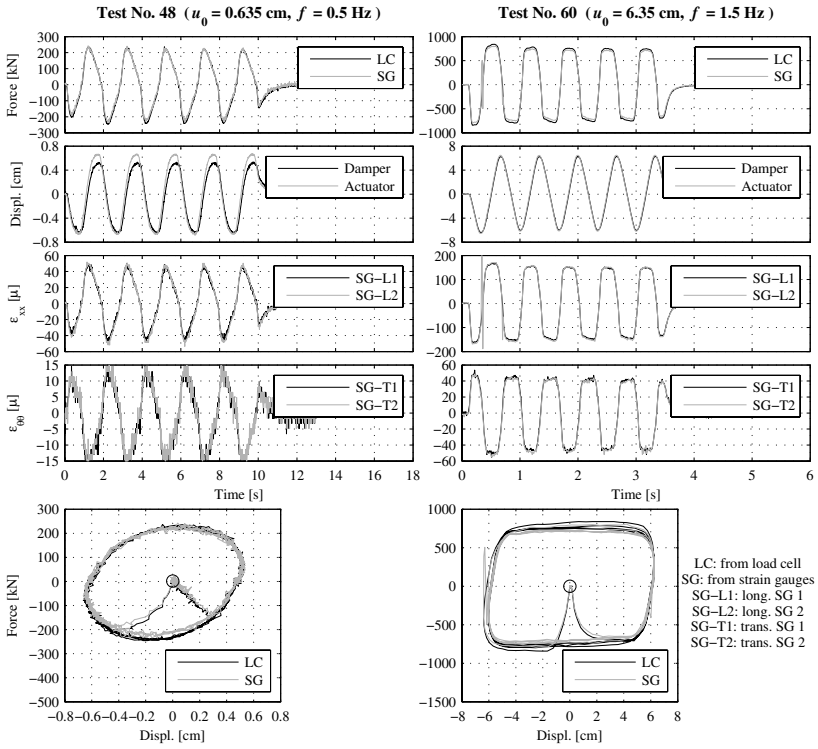

Figure 8. Recorded data from the extender of the 1100-kN damper equipped with weldable strain gauges

3.3. 2000-kN Damper with Weldable Strain Gauges

The following set of indoor tests were conducted on one of the two 2000-kN dampers, equipped with weldable strain gauges. Figure 9 shows selected results from two experiments, the one on the left column from a low-force-output test and the one on the right from a high-force-output test. The top graph shows the force output of the damper. The solid line, designated LC, shows the force recorded using the load cell, while the dashed line, designated SG, shows the force as computed using the recorded strain histories. The average of the longitudinal strain readings from the top and side strain gauges on the extender were used to compute the force, $P = A_e E(\varepsilon_{xx}^{\text{top}} + \varepsilon_{xx}^{\text{side}})/2$, where A_e is the cross-sectional area of the extender (see Table 1).

The second graph from the top on either side shows the velocity of the damper. The solid line shows the velocity history as recorded using a Transtek 0127-0001 velocity transducer, while the dashed line shows the velocity history that results after differentiating the displacement signal obtained using a Novotechnik TLH-1000 position transducer. Note that to obtain a clean velocity signal, after differentiation of the displacement signal, it was necessary to filter the resulting signal. More filtering was necessary for smaller velocity-amplitude motions. Some signal noise was detected even on the data collected using the velocity transducer, which again is more pronounced under low-amplitude excitations. The noise in the directly measured velocity signal is certainly less than the noise in an unfiltered differentiated displacement signal, but filtering is still necessary nevertheless. Since filtering

may be necessary either way, it is perhaps better to simply use one position transducer to measure directly displacement, and obtain the velocity by differentiating and filtering the resulting signal. Details on filtering can be found in Konstantinidis et al. (2012).

The third graph in Fig. 9 shows the displacement history for the test. The solid line shows the displacement recorded using a DCDT attached on the actuator, while the dashed line shows the displacement recorded using the Novotechnik TLH-1000 position transducer attached on the damper. The forth graph shows recorded longitudinal strains, ε_{xx}, from weldable strain gauges attached on the top and side of the extender. The bottom graph shows the hysteretic loops for the test. The solid line shows the force recorded with the load cell versus the damper displacement recorded with the Novotechnik position transducer, while the dashed line shows the force computed from the strain-gauge readings versus the same damper displacement. Figure 9 (bottom) confirms that even for large size dampers with thick extenders, the proposed procedure offers dependable results, even for low-amplitude motions.

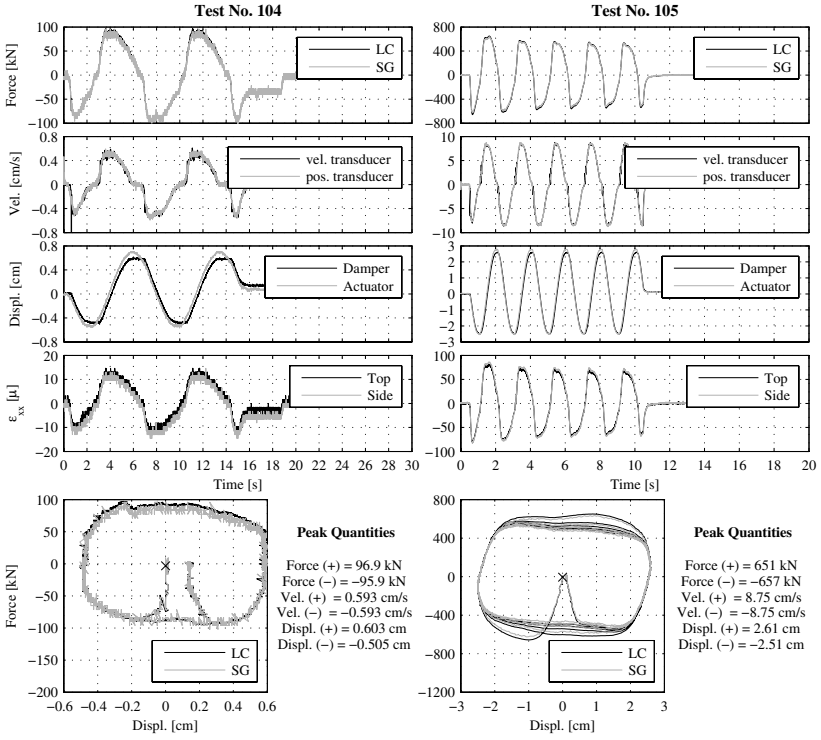

Figure 9. Recorded data from the extender of the 2000-kN damper equipped with weldable strain gauges

3.4. Outdoor Experiments on 2000-kN Damper

The indoor experimental program demonstrated that commercially available strain gauges, either bondable or weldable, can reliably be used to accurately monitor the force output of fluid dampers over a wide range of velocity inputs. It was concluded that gauges should not be placed on the damper casing but rather on the extender piece, preferably near mid-length to avoid end-effects.

Our experimental program proceeded with the testing of the second of the two available 2000-kN dampers on a testing machine that was built for the purposes of this project outside of the testing laboratory at PEER. The purpose of this series of experiments was to investigate possible changes in the force output of the damper over time under service loading conditions, where the frequency and amplitude of the displacement cycles are small. In addition, the damper was instrumented with displacement transducers as well as strain gauges, to examine the effect of environmental conditions on them. In an effort to replicate actual conditions on a bridge, the setup was located very near the bay,

approximate distance 0.5 km, and exposed to wind coming in from the bay.

Figure 2 shows the experimental setup of the outdoor tests, with arrows indicating the locations of the various pieces of instrumentation used. The position transducers used are the Celesco PT5AV and Novotechnik TLH, which were also used in the indoor tests. The Celesco position/velocity transducer was covered with a clear plastic bag, which proved sufficient to keep it operational without problems even during days with massive rainfall. The manufacturer rates the device suitable for wet conditions. In a bridge application, the authors recommend a protective plastic enclosure with holes for the potentiometer wire and connecting cables. It is also recommended that the extended potentiometer wire is slightly inclined so that water that pours on it will trickle away from the device.

Built-up rosettes of weldable strain gauges were attached on the damper extender at its mid-length, one on the top of the extender and one at its side. Vishay Micro-Measurements *M-Coat A*, *M-Coat B*, and *M-Coat J* protective coats. Further details on the outdoor setup and tests can be found in Konstantinidis et al. (2011, 2012)

4. WIRELESS SYSTEM FOR MONITORING OF DAMPERS

A system that utilizes a commercially available portable data acquisition system (Fig. 10) was chosen to collect and transmit data. The data acquisition system, manufactured by Opto 22, can transmit data both wirelessly and/or with wired connections. The device is highly scalable to accommodate a number of channels with different sensor types. Data can be recorded at a wide range of sampling frequencies, and the device is equipped with a buffer memory to save data before an event is triggered.

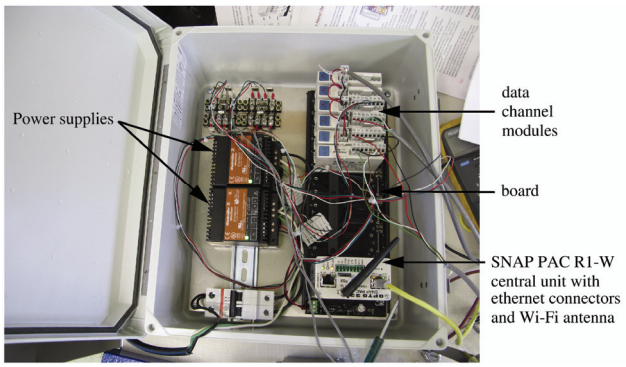

Figure 10. Opto22 system featuring board with central unit with wireless antenna, six channel modules (one displacement, one velocity, and four strain gauge) and two power supplies. The system is protected by a hermetically sealed plastic enclosure box

The system shown in Fig. 10 consists of a integrated board with several slots for data channel modules. As shown, the system features six channels: one for a position sensor, one for a velocity sensor, and four for strain gauges. The central processing unit Opto 22 *SNAP PAC R1-W* has a 10/100 Mbps wired Ethernet network interface and a wireless LAN interface (802.11a, b, and g network standards) to transmit/receive data to/from a remote computer. The PAC Project Basic software or PAC Project Professional can be used to program the SNAP-PAC system to handle a variety of remote monitoring, data acquisition, and control applications. The system can be adapted to accommodate a powerful, external Wi-Fi antenna with a range up to approximately two kilometres, or more. Alternatively, the data may be transmitted to a remote location via a Global System for Mobile Communications (GSM) network (or by its successors, 3G or 4G), although this requires leased telephone lines. More data channels can be easily accommodated on the same board or an expansion board. Two power supplies are included to power the different components of the system. The components of the system are contained within a heavy-duty plastic, hermetically sealed enclosure box, as shown in Fig. 10. Special sealed fittings can be installed on the box in order for wires (e.g., for power) to enter the enclosure.

The Opto 22 was tested on the outdoor 2000-kN damper test setup in parallel with a conventional ATS data acquisition system used commonly at the PEER center test facility at Richmond Field Station, University of California, Berkeley. The Opto 22 system featured one Celesco PT5AV position and velocity transducer, and four 120Ω weldable strain gauges (identical to the ones described in the earlier section). The results of an early test were excellent, with the system being able to reliable acquire and transmit to a remote laptop clean displacement, velocity, and strain-gauge history signals.

The success of the Opto 22 wireless monitoring system in this preliminary phase at the lab brings forward promising opportunities for the system to be tested and adapted to wide applications of health monitoring of fluid dampers in bridges.

5. CONCLUSIONS

The implications of the technology advanced in this paper where the force output of fluid dampers can be monitored in-situ via the use of strain gauges installed on the dampers are outlined below:

- Weldable strain gages are easy to install and can be protected from environmental hazards produced by severe weather, salt-laden atmosphere, and corrosive liquids, such as fuel oil.
- The preferable location of the strain gages on the damper is on the extender element, which experiences the full cycle of tension and compression. It is recommended to install strain gauges in the middle of the extender piece to avoid end effects. Although it is theoretically possible to measure the force using a single longitudinal strain gauge, it is highly recommended to install two strain-gauge rosettes (e.g., one on the top and one on the side of the damper) to provide redundancy but also to be able to capture any undesired shears and moments that may develop in the damper.
- The recorded signals transmitted are noisy and without processing do not allow us to capture the damper forces well. It will be necessary to use a simple filtering algorithm to clean up the signals before computing the damper forces.
- It will be essential before installing a monitoring system on one or more dampers on a bridge to have an estimate of the service-level input that the particular damper will experience. It will be necessary to estimate the damper displacement, velocity (or frequency), and any daily or seasonal variation in these quantities.
- A system that utilizes a commercially available portable data acquisition system manufactured by Opto 22 demonstrated that wireless technology is promising given that data were reliably acquired and transmitted to a remote computer.

ACKNOWLEDGEMENT

Financial support for this study was provided by the California Department of Transportation (Caltrans) under grant 59A0658.

REFERENCES

Delis E.A., Malla R.B., Madani M., and Thompson K.J. (1996). Energy dissipation devices in bridges using hydraulic dampers. *Building to Last, Proceedings of the Structures Congress XIV*. IL, 2, Chicago, IL, 1996; 1188–1196.

Konstantinidis D., Kelly J.M., and Makris N. (2011) In-situ monitoring of the force output of fluid dampers: experimental investigation. *Report No. PEER 2011/103*, Pacific Earthquake Engineering Research Center, University of California, Berkeley, 2011.

Konstantinidis D., Makris N., and Kelly J.M. (2012) Health monitoring of fluid dampers for vibration control of structures: experimental investigation. *Earthquake Engineering and Structural Dynamics* [in press].

Makris N. and Zhang J. (2004). Seismic response analysis of highway overcrossings equipped with elastomeric bearings and fluid dampers. *Journal of Structural Engineering (ASCE*; 130(6):830–845.

Papanikolas P.K. (2002). Deck superstructure and cable stays of the Rion-Antirion bridge. *Proceedings of the 4th National Conference on Steel Structures*, Patras, Greece, 24–25 May 2002.

Zhang J. and Makris N. and Delis T. (2004) Structural characterization of modern highway overcrossings—case study. *Journal of Structural Engineering (ASCE)*; 130(6):846–860.